

The Effects of NCO/OH Ratio on Propylene Oxide-Modified Oil Palm Empty Fruit Bunch-Based Polyurethane Composites

H. D. Rozman, G. S. Tay

School of Industrial Technology, Universiti Sains Malaysia, 11800 Minden, Penang, Malaysia

Received 2 July 2007; accepted 15 June 2008

DOI 10.1002/app.28881

Published online 17 September 2008 in Wiley InterScience (www.interscience.wiley.com).

ABSTRACT: In this study, the effects of NCO/OH ratio on polyurethane composites prepared from propylene oxide-modified oil palm empty fruit bunch (EPB-PO) properties were studied. From the results obtained, the diffusion of solvents in the composites produced was classified as Fickian type. The molecular weight between crosslink points and degree of crosslinking were affected as the NCO/OH was increased. This phenomenon was attributed to the interaction between excess NCO and accessible OH

groups from EPB-PO to form a three-dimensional network. From the mechanical testing results, it was found that the NCO/OH ratio had a significant effect on tensile and flexural test. However, no significant influence was observed on impact strength of the composites produced. © 2008 Wiley Periodicals, Inc. *J Appl Polym Sci* 110: 3647–3654, 2008

Key words: polyurethane; composites; swelling properties; NCO/OH ratio

INTRODUCTION

It is well known that the compatibility between lignocellulosic materials and polymer plays a crucial role in determining the properties of a composite. The interfacial bond strength between lignocellulosic material and polymer is expected if the functional groups present in these two components could be reacted. In thermoplastic-lignocellulosic, coupling agent is employed to create an interfacial region to improve the stress transfer mechanism. Meanwhile, in thermoset-lignocellulosic system, functional groups such as OH group from lignocellulosics could serve as reactive sites to interact with thermoset resin. According to Hatakeyama et al.,¹ natural polymer having more than two hydroxyl groups per molecule could be used as polyol for polyurethane (PU) preparation, if the OH group could react with isocyanate.

Many attempts have been made to utilize natural polymer as raw material for PU synthesis. It could be attributed to its unique features, which can be produced in the form of sheets, foams, adhesives, etc. Hatakeyama et al.¹ attempted several types of lignin, wood meal, and wood tar residue for making PU in the form of sheet, foam, and composites. It was found that plant components could act as stiff

segment in PU system. Previous study also showed that oil palm empty fruit bunch could react with isocyanate in PU composite preparation.² Desai et al.³ had prepared PU adhesives from biomaterial for wood binding. The results showed that it gives superior bondings for wood joints. Wu and Zhang⁴ reported that the starch content showed significant difference to the properties of casting films produced. From the study carried out by Tanaka et al.,⁵ semirigid PU foams could be prepared from palm oil-based polyol up to 80% (w/w). However, its thermal stability decreased with increasing palm oil content. Liquefied wood has been used by Kurimoto et al.^{6,7} to produce PU. From the results obtained, the mechanical properties and the network structure were strongly dependent on the viscosity of the liquefied wood, where higher viscosity gives better properties.

Generally, interfacial properties of these composites could be improved by enhancing the interaction between lignocellulosic materials and polymer. There have been attempts to employ chemical modification on lignocellulosic materials to strengthen this property. Huang and Zhang⁸ prepared PU from nitrolignin, which was synthesized by reacting alkaline lignin with nitric acid and acetic anhydride. The results showed that the introduction of nitrolignin into PU restricted the chain mobility of PU molecules and resulted in a relatively high crosslink structure in the PU formed. On the other hand, Hatakeyama et al.⁹ synthesized PU from saccharide-based polycaprolactone (PCL). They found that the

Correspondence to: H. D. Rozman (rozman@usm.my).

glass transition temperature (T_g) of the PU decreased with increasing caprolactone content that was attached to the saccharide unit. This explanation is in line with the investigation carried out by Tan,¹⁰ where the crosslink density and mechanical properties of PU produced strongly depended on the cardanol content which attached to the lignin molecule.

In this study, the effects of NCO/OH on the properties of EFB-PU composites based on propylene oxide-treated EFB (EFB-PO) were investigated. From the previous study,¹¹ the phthalation results showed that EFB-PO possessed of more OH groups than the native EFB. Thus, further investigations are required to clarify whether different NCO/OH ratio has an effect on the physical properties of the EFB-PU composites prepared from EFB-PO. In this work, EFB-PO with 15% weight percentage gain (WPG) is used. The composites were produced with different NCO/OH ratios that vary from 1.1 to 1.4. The OH value was determined by phthalation as described in previous article.¹¹

EXPERIMENTAL

Preparation

Materials

The EFB in fiber form was obtained from Sabutek Sdn. Bhd. Teluk Intan, Perak, Malaysia. Diphenylmethane diisocyanate (MDI) was supplied by Aldrich Chemical Company (Milwaukee, WI). PEG 200 was obtained from Fluka Chemika (Buchs, Switzerland), whereas PO was supplied by BDH Chemical (Poole, UK).

EFB-PO preparation

The EFB fiber was washed under reflux condition with a solvent mixture [toluene : ethanol : acetone = 4 : 1 : 1 ratio (volume basis)] for 3 h to remove the impurities such as palm oil residues on the fiber surface before grinding. The EFB particles obtained were sieved to separate the particles with different sizes, and only particles with mesh number 35–60 (0.500–0.250 mm) were used in this study. The oven-dried EFB particles were weighed and added into a round bottom reaction flask with 1-L capacity. The PO/EFB = 6 : 1 (eq : eq) ratio was fixed. In this modification, pyridine was used as a solvent as well as a swelling agent. A vigorous stream of nitrogen was applied for 1 min before starting the reaction. The reaction flask was placed in a water bath at 60°C to allow reaction to take place for 24 h. The PO-modified EFB produced was then washed with acetone under reflux condition for 2 h to remove the unreacted chemical reagents. The EFB was then oven-dried at 90°C under pressure before it was used in the composites preparation.

EFB-PU composite preparation

The EFB-PU composite was produced using a one-shot process. First, EFB-PO (oven-dried) was mixed with MDI (according to different NCO/OH ratios) at room temperature followed by the addition of PEG 200 (was dried using molecular sieve type 3 Å). A stream of nitrogen was applied during the mixing process. Mixing was carried out in a water bath at a temperature of 30°C using a mechanical stirrer at 500 rpm for 5 min. Each of the precured EFB-PU was pressed at 125°C for 5 h at a pressure of 500 kg/cm². The sample was postcured in an oven at 125°C for another 24 h.

Characterization

Fourier transform infrared

The EFB-PU composites produced were ground into powder form for Fourier transform infrared (FTIR) analysis. The composite powder was dried and dispersed in dry potassium bromide (ratio of sample:KBr = 1 : 100). The mixture was then pressed into pellets. The samples were run using a Nicolet Avatar 360 FTIR for 64 scans from 4000 to 400 cm⁻¹ wavenumber.

X-ray diffraction

The crystallinity of the dried composite powder was analyzed using Siemens X-ray powder diffractometer model D5000 equipped with a Cu K α target at 40 kV and 20 mA. Diffraction angle ranging from $2\theta = 0^\circ$ to 150° were recorded using a scintillation detector. The area under the peak was considered as the crystallinity of the composite.

Void determination

The void content of the composites produced was determined according to ASTM D 2734-70. First, the theoretical density of each sample was calculated and compared with the measured density. The missing fraction of each sample was considered as void content. The theoretical density of the EFB-PU composites and the void content were calculated by the following equations:

- Theoretical density, T_d

$$T_d = \frac{100}{(\%MDI/\rho_{MDI}) + (\%PEG200/\rho_{PEG200}) + (\%EFB/\rho_{EFB})}$$

where T_d = theoretical density (g/cm³); %MDI = weight percent of MDI; ρ_{MDI} = density of MDI

(1.18 g/cm³); %PEG200 = weight percent of PEG200; ρ_{PEG200} = density of PEG200 (1.12 g/cm³); %EFB = weight percent of EFB (unmodified and modified); ρ_{EFB} = density of EFB (unmodified and modified, g/cm³).

- Void content

$$\text{Void content (\%)} = \frac{T_d - M_d}{T_d} \times 100$$

where T_d = theoretical density (g/cm³); M_d = determined density (g/cm³)

The density of modified EFB was determined in the previous paper.¹¹

Immersion test

This test was conducted according to ASTM 570-77 with sample dimension of 3 × 0.8 × 0.5 cm³ (length × width × thickness). The samples prepared from each EFB-PU composite system were oven-dried for 24 h before being immersed in different solvents [toluene, ethanol, acetone, and *N,N'*-dimethylformamide (DMF)]. The weight and the thickness of the samples were recorded periodically until it became stable. The surface of the composites was blot-dried with absorbent paper before the weight and thickness of the samples were taken. The properties were reported after five measurements for each prepared EFB-PU composite system were taken.

To determine the mode of the sorption (Fickian or non-Fickian) and the mechanism of the sorption, the data obtained was fitted to the following equation^{12,13}:

$$\text{Log } (Q_t/Q_\infty) = \text{Log } k + n \text{Log } t$$

where, Q_t = mole percent of solvent absorb at time t ; Q_∞ = mole percent of solvent absorbed at equilibrium; k = a constant.

The values of n and k were determined by linear regression analysis.¹⁴⁻¹⁶ According to Harogappad and Aminabhavi,¹² the k value gives an idea about the extent of the polymer-solvent interaction and n value decides the mode of sorption mechanism. Diffusion (D) of a solvent in composite could be determined by the equation shown below,¹⁵⁻¹⁷

$$D = \pi/16(h\theta/Q_\infty)^2$$

where h = initial thickness of the samples; θ = slope of the graph of Q_t against $t^{1/2}$ before 50% sorption.

Sorption coefficient is related to the maximum sorption of the solvent that can be obtained from the ratio of weight of the solvent absorbed at equilibrium stage to the initial weight of the polymer.¹⁴ The sorption coefficient (S) of the EFB-PU composites can be calculated using equation shown below^{15,16}:

$$S = M_s/M_p$$

where M_s = mass of solvent absorbed at equilibrium swelling (in gram); M_p = mass of the composite at initial state (in gram).

The permeability of the EFB-PU composites could be expressed by permeability coefficient (P), which could be calculated as shown^{15,16}

$$P = DS$$

The swelling coefficient (α) could be obtained using equation shown below. The solubility parameter of each series of EFB-PU composites could be obtained when the maximum swelling was achieved,^{14,18}

$$\alpha = (M_s/M_p) \times (1/\rho_s)$$

where M_s = mass of the solvent in the swollen sample at equilibrium (in gram); M_p = mass of the composite at initial state (in gram); ρ_s = density of the respective solvent (g/cm³).

Polymer-solvent interaction parameter (χ) of each type of composites was determined using equation shown below:

$$\chi = \beta + V_s[(\delta_p - \delta_s)^2/RT]$$

where β = lattice constant, 0.34; V_s = molar volume of solvent, cm³/mol; δ_p = solubility parameter of composite (cal/cm³)^{1/2}; δ_s = solubility parameter of the solvent (cal/cm³)^{1/2}; R = gas constant, 1.983 cal/(mol K); T = temperature, K.

Molecular weight between crosslink points (M_c) and degree of crosslinking

M_c is defined as the average of molecular weight of chain between two crosslink sites, whereas degree of crosslinking (DC) refers to the extent of the crosslink per unit weight polymer qualitatively. Low DC indicates relatively few crosslinks per unit weight of polymer. High DC indicates relatively high crosslink content per unit weight of polymer. In this study, the M_c and DC were determined using the following equations^{14,19}:

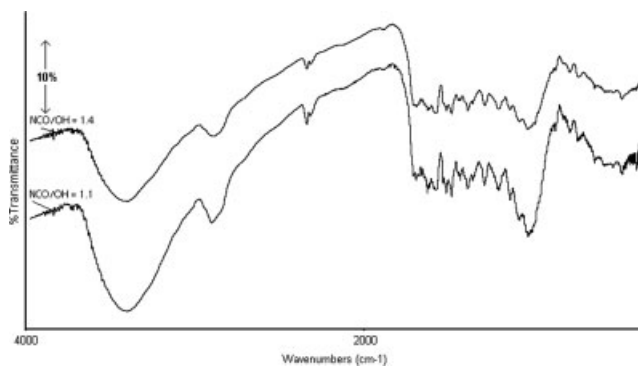


Figure 1 The infrared spectra of composites with EFB-PO in different NCO/OH ratios.

- Molecular weight between crosslink points (M_c)

$$M_c = -(\rho_p V_s \Phi^{1/3}) / (\ln(1 - \Phi) + \Phi + \chi \Phi^2)$$

- Volume fraction (Φ)

$$\Phi = \frac{M_p / \rho_p}{(M_s / \rho_s) + (M_p / \rho_p)}$$

where M_s = mass of the solvent in the swollen sample at equilibrium (in gram); M_p = mass of the composite at initial state (in gram); ρ_s = density of DMF (g/cm^3); ρ_p = density of the respective EFB-PU composites (g/cm^3); V_s = molar

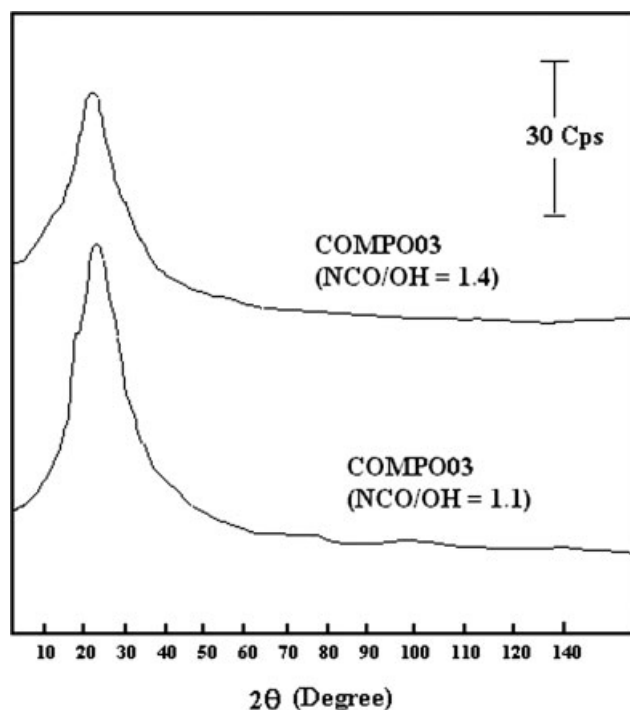


Figure 2 The diffractograms of composites with EFB-PO in different NCO/OH ratio.

TABLE I
Crystallinity of EFB-PU Composites Prepared from EFB-PO at Different NCO/OH Ratios

Composites (NCO/OH)	Crystallinity (%)
1.1	24.07
1.2	22.39
1.3	19.66
1.4	17.92

volume of solvent, cm^3/mol ; χ = polymer-solvent interaction parameter.

- Degree of crosslinking (ν)

$$\nu = 1/2M_c$$

Mechanical testing

Tensile test

The composites produced were cut into tensile test specimens. Tensile test was carried out according to ASTM D3039 on samples with a dimension of $12 \times 0.8 \times 0.5 \text{ cm}^3$ (length \times width \times thickness) using Instron Testing Machine model 5582, with cross-head speed of 5 mm/min. The properties were reported based on five measurements for each EFB-PU composite system. Properties such as strength, modulus, elongation at break, and toughness were obtained from this test. The specific tensile properties were calculated by normalizing the tensile result obtained with the corresponding sample density.

Flexural test

The flexural test (three-point bending) was conducted according to ASTM D 790 with the sample dimension of $10 \times 0.8 \times 0.5 \text{ cm}^3$ (length \times width \times thickness). The samples were tested using Instron Testing Machine model 5582 at a cross-head speed of 2 mm/min. The properties were reported after six measurements for each EFB-PU composite system were taken and properties such as strength, modulus, and toughness were computed. The specific flexural properties were calculated by normalizing the flexural result with the corresponding sample density.

TABLE II
Densities (Theoretical and Determined) of EFB-PU Composites Prepared from FB-PO with Different NCO/OH Ratios

Composites (NCO/OH)	Theoretical (g/cm^3)	Determined (g/cm^3)	Void content (%)
1.1	1.17	1.02	12.8 (± 0.64)
1.2	1.18	1.03	12.7 (± 0.32)
1.3	1.18	1.03	12.7 (± 0.43)
1.4	1.18	1.04	11.9 (± 0.38)

TABLE III
The n and k Value of the Composites with EFB-PO in Different NCO/OH Ratios in Various Types of Solvent

Samples (NCO/OH)	DMF		Toluene		Acetone		Ethanol	
	n	k (10^{-3})	n	k (10^{-3})	n	k (10^{-3})	n	k (10^{-3})
1.1	0.54	6.37	0.62	3.74	0.54	7.62	0.57	4.20
1.2	0.54	8.29	0.57	5.03	0.57	5.38	0.52	4.42
1.3	0.50	9.78	0.57	4.63	0.59	4.19	0.58	2.80
1.4	0.53	7.43	0.56	4.84	0.53	6.42	0.53	4.42

Impact strength

Impact test was carried out using Pendulum Tester Model 5101 (Charpy method) with sample dimension of $6.5 \times 0.8 \times 0.5 \text{ cm}^3$ (length \times width \times thickness). The pendulum energy of 2 J was used for all the samples. The test was conducted according to ASTM D 256 with six replicates. The impact strength of the sample was calculated. Again, the specific impact strength was calculated by normalizing the impact strength with the corresponding sample density.

RESULTS AND DISCUSSION

Characterization

Figure 1 depicts the FTIR spectra of composites with NCO/OH of 1.1 and 1.4, respectively. It can be seen that the absence of absorption at about 2280–2260 cm^{-1} designated to isocyanate shows that all added isocyanate have been consumed in the preparation of composites. Thus, it shows that the newly generated OH groups have interacted with the isocyanate in the formation of a three-dimensional network. By looking at the crystallinity result shown in Figure 2, the composite with higher NCO/OH ratio shows a broader peak as compared with the composite with lower NCO/OH. Table I depicts the area under peak of the diffractograms shown in Figure 2. It is clearly seen that the sample with a higher NCO/OH ratio exhibits lower crystallinity, indicative of the existence of a more amorphous structure. According to Canche-Escamilla et al.,²⁰ grafting an amorphous polymer (PMMA) onto a lignocellulosic material would reduce the crystallinity of the grafted fiber. Hence, this result indicates that MDI was chemically attached to the EFB-PO resulting in a reduction in

the crystallinity, due to the fact that MDI amount was increased with the increment of NCO/OH that generally considered an amorphous material. Thus, this would surely reduce the crystallinity of the composite.

Table II shows the densities and void contents of composites prepared from EFB-PO with various NCO/OH ratios. From the results obtained, the determined densities are slightly lower than the theoretical ones. This could be attributed to the voids generated by carbon dioxide that was released via the interaction between the isocyanate and the environment water vapor during the mixing process. However, no apparent correlation is observed between the increments of NCO/OH ratios with the resultant void content.

Immersion test and M_c determination

For immersion test, the mode of sorption (n) and the k values calculated with a linear regression analysis are presented in Table III. From the results shown, the n values are found to vary in the range of 0.50–0.62, indicative of a Fickian type sorption mechanism. Hence, the sorption kinetic in all types of solvent is found to depend on the concentration of solvent and immersion time. On the other hand, k value, a quantitative index of interaction between composites and solvent shows no significant trend with variation in NCO/OH ratio.

The diffusion coefficient (D), sorption coefficient (S), and permeability coefficient (P) values of the composites immersed in the solvents are depicted in Tables IV and V. In DMF, the S and P are found to decrease with increment in NCO/OH ratio. These phenomena could be explained by an established

TABLE IV
The D , S , and P of Composites from EFB-PO with Different NCO/OH Ratios in DMF and Toluene

Composites (NCO/OH)	DMF			Toluene		
	$D \times 10^{-5}$ (cm^2/s)	S	$P \times 10^{-5}$ (cm^2/s)	$D \times 10^{-5}$ (cm^2/s)	S	$P \times 10^{-5}$ (cm^2/s)
1.1	26.6 (± 2.7)	1.67 (± 0.11)	44.4 (± 6.1)	20.60 (± 2.11)	0.19 (± 0.01)	3.81 (± 0.47)
1.2	33.1 (± 6.8)	1.52 (± 0.10)	50.4 (± 11.1)	27.70 (± 0.68)	0.15 (± 0.01)	4.05 (± 0.19)
1.3	32.6 (± 8.6)	1.32 (± 0.10)	43.1 (± 2.2)	24.50 (± 0.88)	0.12 (± 0.01)	3.05 (± 0.23)
1.4	28.6 (± 1.0)	1.33 (± 0.05)	38.1 (± 1.9)	25.70 (± 1.04)	0.13 (± 0.01)	3.35 (± 0.17)

TABLE V
The D , S , and P of Composites from EFB-PO with Different NCO/OH Ratios in Acetone and Ethanol

Composites (NCO/OH)	Acetone			Ethanol		
	$D \times 10^{-5}$ (cm ² /s)	S	$P \times 10^{-5}$ (cm ² /s)	$D \times 10^{-5}$ (cm ² /s)	S	$P \times 10^{-5}$ (cm ² /s)
1.1	29.40 (± 2.21)	0.26 (± 0.03)	7.46 (± 0.92)	15.20 (± 1.25)	0.24 (± 0.03)	3.61 (± 0.47)
1.2	143.00 (± 2.32)	0.23 (± 0.01)	34.50 (± 1.72)	7.91 (± 1.18)	0.24 (± 0.01)	1.90 (± 0.25)
1.3	133.00 (± 5.71)	0.21 (± 0.01)	27.80 (± 1.74)	7.68 (± 0.17)	0.22 (± 0.02)	1.66 (± 0.15)
1.4	106.00 (± 1.99)	0.22 (± 0.02)	23.00 (± 2.42)	8.22 (± 0.49)	0.22 (± 0.01)	1.81 (± 0.10)

network formed in the composites resulted from the three-dimensional network formation with excess isocyanate, which restricts the penetration of DMF. This is supported by the result observed in FTIR analysis. As a result, the capability to absorb DMF decreased with the increase in NCO/OH ratio. However, no apparent change is observed in D value. As shown in Table II, no significant difference is observed in the void content among the composites produced that could be attributed to an identical diffusivity of DMF among the composites. The results also show that all composites absorb relatively lower amount of toluene, acetone, and ethanol than DMF. In other words, DMF shows the highest capability to penetrate into the composites. This indicates that the solubility parameter of the EFB-PU composites prepared from different NCO/OH ratios is close to the solubility parameter of DMF which is $12.3 \text{ (cal/cm}^3)^{1/2}$.

From Tables IV and V, no significant trend of D is observed as a function of NCO/OH ratios in toluene and ethanol, except those immersed in acetone. According to Elias,²¹ PU prepared from polyethylene glycol and MDI could dissolve in acetone. Hence, these results show that PU matrix has a higher affini-

ty to acetone, which could be due to the increase of matrix portion resulted from the increase in MDI amount. However, in this study, no obvious solubility in acetone is evident.

The solubility parameter of the composites prepared was determined by plotting the swelling coefficient of composite as a function of solubility parameter obtained from a series of solvents as depicted in Figure 3. Generally, the maximum swelling coefficient is observed to fall within the range of 11.0 to 12.0. By differentiating the equation shown in the figure, the solubility parameter of composite can be calculated, which is 11.6, and the χ values for the composites in each solvent are shown in Table VI. To select the appropriate χ value in the M_c and DC calculation, various factors need to be taken into consideration. According to Flory-Huggins theory, value of χ must be less than 0.5 to obtain a completely miscible system.¹⁸ Thus, the results obtained indicate that toluene and acetone are not a suitable solvent in this case. The relative swelling of lignocellulosic material in various types of solvent must be considered in the selection of χ . According to Stamm,²² the relative swelling of lignocellulosic

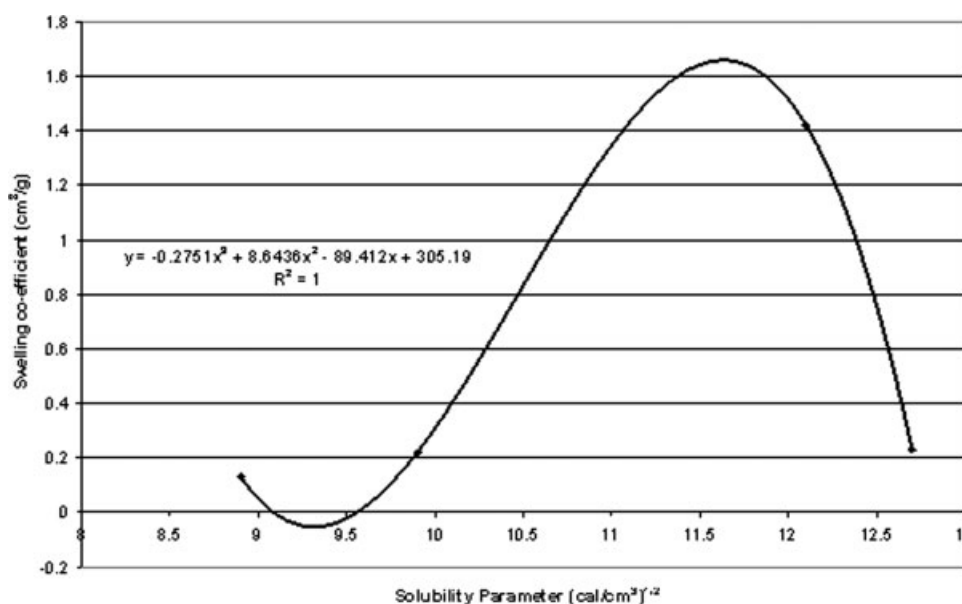


Figure 3 Swelling coefficient versus solubility parameter of solvents for EFB-PU composites prepared from EFB-PO with NCO/OH ratio = 1.2.

TABLE VI
Polymer–Solvent Interaction Parameter (γ) for EFB-PU
Composites Prepared from EFB-PO with Different
NCO/OH Ratios in Various Types of Solvent

Composites (NCO/OH)	Ethanol	Toluene	DMF	Acetone
1.1	0.46	1.64	0.37	0.70
1.2	0.46	1.64	0.37	0.70
1.3	0.46	1.64	0.37	0.70
1.4	0.46	1.64	0.37	0.70

materials in toluene, acetone, and ethanol are 0.016, 0.63, and 0.83 respectively. This shows that the swelling of the EFB in toluene, acetone, and ethanol is relatively lower than in DMF (1.23). In other words, the DMF demonstrates highest swelling coefficient as compared with the others. Thus, DMF and EFB-PU composites are miscible with a χ value of 0.37. This value is in agreement with Yoshida et al.²³ who prepared PU composite from Kraft lignin.

Figure 4 depicts the M_c and DC against different NCO/OH ratios. From the results obtained, the DC increases with progressive increase in NCO/OH ratio. This observation has led to the explanation that the addition of isocyanate could have enhanced the formation of a three-dimensional network by reacting with those newly generated OH groups produced from the reaction between PO and EFB.¹¹ According to the studies carried out by Yoshida et al.²³ and Saraf and Glasser,²⁴ excessive isocyanate over OH groups could help to produce a composite with a higher crosslink density through allophanate and biuret linkages. Hence, this explains why a

reduction is observed in M_c that in turn accounts for the reduction in swelling properties, as the NCO/OH ratio is increased. In short, the reduction in M_c with a higher NCO/OH ratio has resulted in a restriction in the molecules mobility in EFB-PU composite due to the formation of a three-dimensional network. Again, this result also explains the decreasing trend observed in DMF sorption (S).

Table VII presents the tensile properties of EFB-PU composites with different NCO/OH ratios. It can be seen that the tensile strength and toughness increase as the NCO/OH ratio is increased. From the previous results (Table I and Fig. 4), a reduction in crystallinity and an increment in DC are observed as the NCO/OH ratio is increased. In this context, it is generally believed that the effect of DC is found to be more pronounced than crystallinity in determining the tensile properties of the EFB-PU composites prepared. Therefore, the increase in tensile strength and toughness with progressive increase in NCO/OH ratio is caused by an increase in DC. In addition, the observed phenomenon could also be attributed to the reduction in the exposed OH groups that generally serve as stress concentration points.² As a result, a better adhesion between EFB-PO and PU matrix may have improved the stress transfer from the PU matrix to the EFB-PO. As a result, a higher energy is required to bring the sample to failure.

On the other hand, the tensile modulus of the composites shows a slight increase as NCO/OH ratio is increased. This could be due to a shorter chain length within crosslink points, which restricts the mobility of molecules when stress is applied. In other words, the rigidity of composite is slightly increased as the

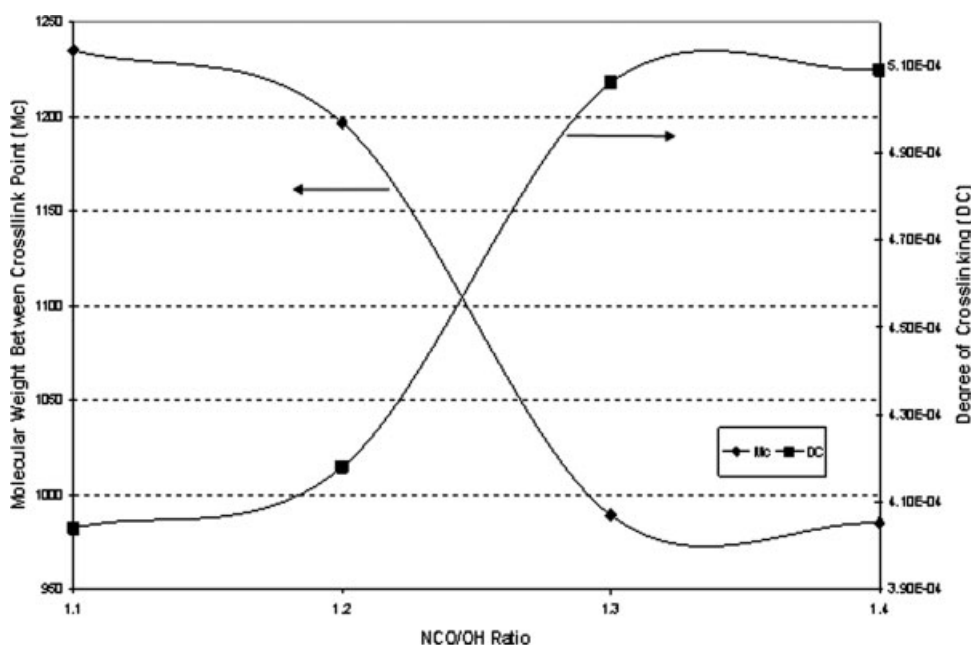


Figure 4 Influence of NCO/OH ratio on molecular weight between crosslink point and degree of crosslinking of EFB-PU composites prepared from EFB-PO.

TABLE VII
Tensile Properties of Composites from EFB-PO with Different NCO/OH Ratios

Composites (NCO/OH)	Specific tensile strength (MPa)	Specific tensile toughness (kJ/m ²)	Specific tensile modulus (GPa)	Elongation at break (%)
1.1	13.85 (±0.7)	4.44 (±0.3)	2.25 (±0.4)	1.11 (±0.06)
1.2	17.21 (±1.0)	8.37 (±0.5)	2.28 (±0.05)	1.12 (±0.06)
1.3	17.46 (±0.8)	8.76 (±0.5)	2.40 (±0.08)	1.08 (±0.04)
1.4	21.40 (±0.8)	11.81 (±0.4)	2.50 (±0.06)	1.09 (±0.04)

NCO/OH ratio is increased. As for the elongation at break, no significant trend is observed.

Table VIII shows the flexural properties of the composites prepared with different NCO/OH ratios. A similar trend as shown in tensile properties is observed. Hence, the same explanation probably holds in this regard. It can be explained that more energy is needed to fail the composites prepared with a higher NCO/OH ratio. This phenomenon is resulted from a better interfacial property that has been introduced into the composites when a higher NCO/OH ratio is employed. For flexural modulus, it also increases with increasing NCO/OH ratio. According to Yoshida et al.²³ this could be attributed to the introduction of aromatic rings from MDI to the matrix, which serves as a hard segment within the PU composites. In addition, the increase of stiffness in the composites produced may also be attributed to the decrease in M_c .

Table IX depicts the impact strength of the composites produced with different NCO/OH ratios. It seems that no significant difference is observed. This is in line with the results shown in the elongation at break analysis. Hence, this observation reveals that the enhanced three-dimensional network of EFB-PU composites prepared from higher ratio of NCO/OH is not sufficient to resist high-speed impact stress.

CONCLUSIONS

This study showed that the increment of NCO/OH ratio can affect the properties of EFB-PU composites produced from EFB-PO. With higher MDI amount,

TABLE VIII
Flexural Properties of Composites from EFB-PO with Different NCO/OH Ratios

Composites (NCO/OH)	Specific flexural strength (MPa)	Specific flexural toughness (kJ/m ²)	Specific flexural modulus (GPa)
1.1	35.88 (±1.52)	1.86 (±0.13)	3.43 (±0.14)
1.2	40.07 (±1.13)	2.41 (±0.15)	3.51 (±0.08)
1.3	40.25 (±0.91)	2.47 (±0.11)	3.63 (±0.12)
1.4	42.07 (±0.82)	2.75 (±0.12)	3.72 (±0.05)

TABLE IX
Impact Strength of Composites from EFB-PO with Different NCO/OH Ratios

Composites (NCO/OH)	Specific impact strength (kJ/m ²)
1.1	9.31 (±0.7)
1.2	10.66 (±0.5)
1.3	10.82 (±0.4)
1.4	11.99 (±0.5)

the mechanical properties of the composites were improved, except for impact strength. M_c was reduced while DC was increased as the NCO/OH ratio was increased. This will create more interaction between EFB-PO and matrix at interface region where stress transfer can occur, which in turn restricts the DMF penetration.

References

- Hatakeyama, H.; Hirose, S.; Nakamura, K.; Hatakeyama, T. *In Cellulosics: Chemical, Biochemical and Material Aspects*; Kennedy, J. F.; Phillips, G. O.; Williams, P. A., Eds.; Ellis Horwood: New York, 1993; p 525.
- Rozman, H. D.; Tay, G. S.; Abubakar, A.; Kumar, R. N. *Eur Polym J* 2001, 37, 1759.
- Desai, S. D.; Patel, J. V.; Sinha, V. K. *Int J Adhes Adhes* 2003, 23, 393.
- Wu, Q.; Zhang, L. *J Appl Polym Sci* 2001, 79, 2006.
- Tanaka, R.; Asano, Y.; Hirose, S.; Hatakeyama, H.; Hatakeyama, T. *Preparation and Thermal Analysis of Palm Oil-Based Polyurethanes*, in 12th International Symposium on Wood and Pulping Chemistry, Madison, Wisconsin, USA, June 9–12, 2003.
- Kurimoto, Y.; Takeda, M.; Koizumi, A.; Yamauchi, S.; Doi, S.; Tamura, Y. *Bioresour Technol* 2000, 74, 151.
- Kurimoto, Y.; Takeda, M.; Doi, S.; Tamura, Y.; Ono, H. *Bioreour Technol* 2001, 77, 33.
- Huang, J.; Zhang, L. *Polymer* 2002, 43, 2287.
- Hatakeyama, H.; Izuta, Y.; Kobashigawa, K.; Hirose, S.; Hatakeyama, T. *Macromol Symp* 1998, 130, 127.
- Tan, T. T. M. *Polym Int* 1996, 41, 13.
- Tay, G. S.; Rozman, H. D. *J Appl Polym Sci* 2007, 106, 1697.
- Harogopad, S. B.; Aminabhavi, T. M. *Polymer* 1990, 31, 2346.
- Unnikrishnan, G.; Thomas, S. *Polymer* 1994, 35, 5504.
- Desai, S.; Thakore, I. M.; Devi, S. *Polym Int* 1998, 47, 172.
- Sreekala, M. S.; Kumaran, M. G.; Thomas, S. *Compos A* 2002, 33, 763.
- Sreekala, M. S.; Thomas, S. *Compos Sci Technol* 2003, 63, 861.
- Aithal, U. S.; Aminabhavi, T. M. *J Appl Polym Sci* 1991, 42, 2837.
- Rosen, S. L. *Fundamental Principles of Polymeric Materials*, 2nd ed.; Wiley: New York, 1993.
- Jacob, M.; Thomas, S.; Varughese, K. T. *Compos Sci Technol* 2004, 64, 955.
- Canche-Escamilla, G.; Cauich-Cupul, J. I.; Mendizabal, E.; Puig, J. E.; Vazquez-Torres, H.; Herrera-Franco, P. J. *Compos Part A: Appl Sci Manuf* 1999, 30, 349.
- Elias, H. G. *Theta Solvents*. *Polymer Handbook*; Brandrup, J.; Immergut, E. H., Eds.; Wiley: New York, 1989; p VII/291.
- Stamm, A. J. *Wood and Cellulose Science*. The Ronald Press Company: New York, 1964.
- Yoshida, H.; Morck, R.; Kringstad, K. P.; Hatakeyama, H. *J Appl Polym Sci* 1987, 34, 1187.
- Saraf, V. P.; Glasser, W. G. *J Appl Polym Sci* 1984, 29, 1831.